Supplementary information

Laser set-up

The fibre laser cavity used in this work consisted of a loop and an open-ended section (cf. Fig. 2 and in more detail in Fig. SI 1). Gated amplification was provided inside the loop by driving with current pulses a semiconductor optical amplifier, Thorlabs SOA 1013SXS. A 125 m delay fibre was also included in the loop to increase the round-trip time of the cavity to the ~1 µs range. In some experiments, particularly with very short-duration pulses, a commercial erbium-doped fibre amplifier (EDFA Thorlabs 100S) was also inserted in the loop. It amplified the weak backscattered signal from the distributed mirror by up to ~36 dB before the SOA. When the extra EDFA was included, an adjustable spectral filter (Alnair-Labs-CVF-300CL) was also used to reduce the amplified spontaneous emission, and limit the feedback signal to the neighbourhood (<20 GHz) of the wavelength of interest. The 3 dB fused fibre coupler connected the loop to the open-ended fibre section of the cavity. A large fraction of the amplification needed for the laser to go above threshold (54.5 dB) was provided by a 27 m long Corning erbium-doped fibre (1550C3) without isolators, working in both directions. Gain was provided to the EDF by a 365 mW CW-pumped diode laser at 976 nm wavelength. An open-ended 63-m long spool of single-mode fibre completed the laser cavity. The output of the laser was monitored with a 26 GHz amplified photodiode model UPD-15-IR2-FC and a 3.5 GHz 40 GSamples/s Tektronix DPO7354 oscilloscope. The spectrum of the laser output was measured with an Apex AP2050A optical spectrum analyser with an optical frequency resolution as narrow as 20 MHz (0.16 pm wavelength). The current pulses for the SOA were provided by an Avtech pulse generator (AVM-2) delivering up to 300 milliamperes with a rise time <1ns and durations up to 20 ns. The trigger for the pulse generator came from a two-channel Keysight arbitrary function generator Model 33500B which allowed for pulse frequency tuning to the millihertz resolution. The short section of fibre providing for Rayleigh backscattering was chosen in position and in length along the fibre spool by adjusting the repetition rate and the duration of the electrical pulses driving the SOA. The single-mode fibre end was angle-cleaved and bent sharply to prevent backscattering from the termination. Lasing was observed along the entire spool length, but the pulse amplitude and stability varied because of the random feedback.

When measuring temperature, a section of the single-mode fibre was attached to the bottom of a polystyrene box containing approximately 3 litres of water. Two 4.5 digits thermometers and one thermocouple were also attached to its bottom inner surface. The voltage from the type k (Chromel-Alumel) thermocouple was monitored with a microvoltmeter HP 34401A. A preliminary calibration of the thermocouple gave a linear 40 µV/K voltage dependence in the limited temperature range studied, simulating a possible dam monitoring temperature range. The resolution of the microvoltmeter and the uniformity of the temperature of the water bath were the main limiting factors in the determination of the temperature displayed in Fig. 5. Increased accuracy of the measurement would require calibration of the temperature against a fixed and known value such as the fusion point of ice. Such a procedure was not carried out in this proof-of-concept experiment.

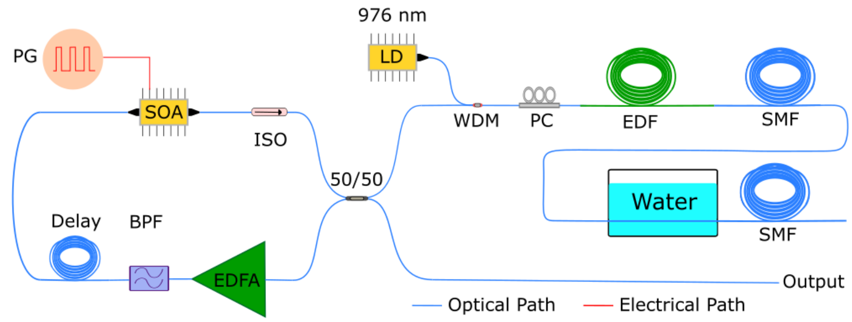

Fig. SI 1. Schematic diagram of distributed temperature sensing using Rayleigh scattering in single-mode telecom fibre. Transform-limited pulse generation makes the laser system highly spectrally efficient. Here, 9.0 cm resolution and 3.3×10^{-3}K precision were demonstrated.

Gain measurements, threshold

The loss of individual components and connectors and the gain provided by the amplifiers were evaluated to better understand the gain dynamics and the limits of operation of the laser. In its simplest configuration of Fig. 2, dispersion shifted (DS) fibre was used. The total loss from all components splices and connections was 11 dB, including the 6-dB double pass over the coupler, whereas the maximum roundtrip-gain was found to be 69 dB, with 54.5 dB coming from the double-pass in the pumped EDF and 14.5 dB from the single-pass at the SOA. Naturally, the highest loss of the cavity was at the distributed back reflector, which amounts to the mean value of ~ -72 dB/m for a typical single-mode fibre and -69 dB/m for DS fibre. With 10-ns pulses in the DS fibre, the laser reached threshold near the maximum gain, meaning that a coherent reflectivity spike ~11 dB was available within the ~250 GHz (~2 nm) spectral region of maximum gain of the pumped EDF. Laser pulses in a standard fibre or shorter laser pulses in the DS fibre could only be observed by increasing the maximum gain, which was obtained by adding a commercial EDFA into the loop and a band pass filter to limit the ASE input on the SOA as displayed in Fig. SI 1. This configuration provided a maximum gain of 105 dB, which was comfortable to generate lasing pulses with durations down to ~0.3 ns, electronics limited. Furthermore, reducing the available spectral width to a flat-top 20 GHz band allowed for better stability of the laser.

Electrical vs optical pulses

The optical pulses generated by the SOA are shorter than the current pulses used for driving it, as shown in Fig. SI 3, for 10-ns (left) and 3-ns (right) bias. The optical pulses measured have duration 8.6 and 1.6-ns FWHM, respectively. The exact relative timing between the electrical and optical pulses is unknown. The figure shows that the response of the SOA in an open cavity (no optical feedback) and the signal-to-noise ratio is relatively poor because of the low sensitivity and high noise level of the ultrafast photodiode. Fig. SI 2 illustrates how sub-nanosecond optical pulses can be formed for current pulses <2 ns, and also that the shape of the optical pulse generated for the shortest durations deviates significantly from a top-hat function.

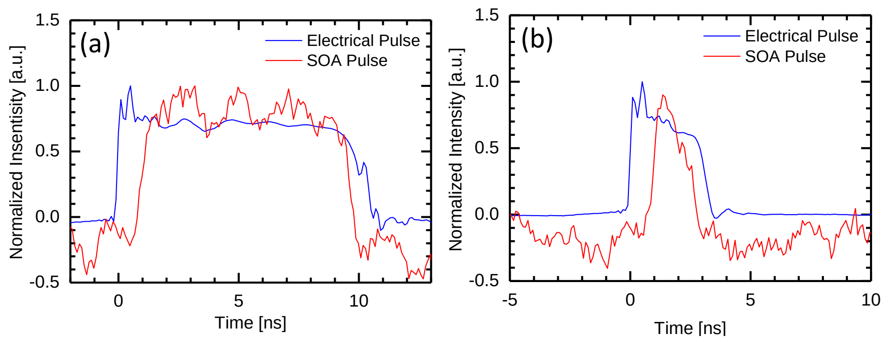

Fig. SI 2. Oscilloscope traces of current pulses applied to the SOA (blue traces) and correspondent optical signals (red traces) with the optical cavity opened. (a) 10.ns current pulse; (b) 3-ns current pulse.

Temperature measurements

In the proof-of-concept application discussed here, the temperature of the water tank was initially raised to ~40°C and the liquid stirred. Subsequently, the polystyrene lid was closed, and the system's temperature left to gradually reduce. The cooling process took several hours. The spectral acquisition and data recording took a fraction of a minute between measured points. The range of temperatures measured was chosen to be a representative temperature at a realistic warm dam location, to allow for the temperature to be in quasi-equilibrium, and to allow for data recording before the electronics instrumentation for temperature measurements showed any variation. The error bar in the temperature measurements is ±0.0125 K. Higher precision would have been possible with better instrumentation (e.g., a nanovoltmeter to read the voltage of the immersed thermocouple).

Fig. SI 3 exemplifies two spectra measured of 900-ps laser pulses with the optical feedback provided by the backscattering fibre section immersed in the water tank. The blue and red traces show spectra at a temperature difference of 0.13 ^{o}C. It is clear that the entire spectrum shifts with temperature, but this shift is better quantified by determining the centre position of the laser line using a Gaussian fit, considering the 70% upper part of the signal to minimise the influence of noise. The error in the determination of the peak frequency was the standard error provided by the Levenberg-Marquardt fitting algorithm and is clearly more precise than the simple determination of the maximum, which was much more affected by the noise. The spectral peak of the two data sets can be determined with a precision ~3 MHz, corresponding to a temperature 2.5 mK. The sensitivity of the technique was evaluated by considering the quality of the least squares fit over 24 independent measurements. The average R2-value was 0.975±0.015 while the standard error in the position of the laser line was 3.2 MHz ±750 kHz, so that the overall sensitivity of a typical spectral position in this case should be ~4 MHz or 3.3 mK in this 9 cm fibre section. Indeed, a longer fibre section used to determine the average temperature would provide sharper spectral lines whose frequency could be determined with even better precision, but the spatial resolution would be compromised accordingly. This distributed temperature measurement is Fourier Transform limited: $\Delta z \times \Delta T = 3\text{x}10^{-4}$ m.K.

It is worth stressing that the accuracy of the measurements is significantly poorer, since the two thermometers employed for absolute measurements were not calibrated against a good temperature reference. Nevertheless, in field-applications, it is often the temperature deviation from the expected value, from for example neighbouring points, daily and seasonal variations, etc., that is most useful.

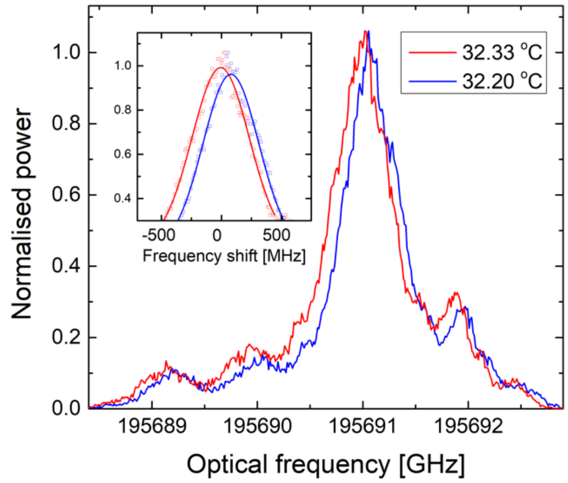

Fig. SI 3. Spectra of 900-ps optical pulses measured at close temperatures The inset displays the Gaussian fit to the 70% upper part of the spectrum, used in the determination of the central frequency.

Acknowledgments

The authors thank J. Murray and B. Redding (NRL, Washington DC) for useful discussions. Funding from CNPq (403233/2017-8, 306332/2019-1, 140701/2019-2), FAPERJ (E-26/201.200/2021), National Institute of Photonics - INCT de Fotônica (465.763/2014-6), Office of Naval Research Global (N62909-20-1-2033), K. A. Wallenberg Foundation and Swedish Research Council are gratefully acknowledged.